Letters in Applied NanoBioScience
Open-Access Journal (ISSN: 2284-6808)

Article
Volume 15, Issue 1, 2026, 7
https://doi.org/10.33263/LIANBS151.007

Separation of B, Al, Ga by Germanium Carbon-based Nanocage: Characterization, Functionalization, and Physicochemical Studies by DFT Insight

Fatemeh Mollaamin [1,*], Majid Monajjemi [2]

1 Department of Biomedical Engineering, Faculty of Engineering and Architecture, Kastamonu University, Kastamonu, Turkey
2 Department of Biology, Faculty of Science, Kastamonu University, Kastamonu, Turkey
* Correspondence: fmollaamin@kastamonu.edu.tr;

Received: 4.10.2025; Accepted: 5.02.2026; Published: 30.03.2026

Abstract: Non-metal and Metal atoms adsorbed into the germanium carbide (GeC) nanocage system were investigated by first-principles calculations. GeC was created and studied as an anode material used to absorb boron (B), aluminum (Al), and gallium (Ga) inside biological cells, forming nanoclusters like "B_2(GeC), Al_2(GeC), and Ga_2(GeC)". A comprehensive investigation into these "B_2(GeC), Al_2(GeC), and Ga_2(GeC)" complexes was conducted using computational methods, focusing on charge density differences (CDD), total density of states (TDOS), and molecular electrostatic potential (ESP) for these hybrid nanoclusters. The basis of the metal–nonmetal interaction is the presence of topological and structural defects, as well as heteroatom functional group silicon that breaks the perfect symmetry of a graphene layer, providing preferential nucleation and growth sites for metal nanoparticles and a single metal site. B_2(GeC), Al_2(GeC), Ga_2(GeC) nanoclusters have shown the steepest maximum TDOS surrounding –0.40, –0.50, and –0.60 a.u. owing to the covalent bond between B, Al, Ga atoms and GeC nanostructure with a maximum density of states of ≈ 12. Functionalizing of Li, B, Al, Ga atoms can augment the negative atomic charge of C2, C3, C7–C12, C14, C15, C17, C18, C22–C27, C29, C30 as electron acceptors in B_2(GeC), Al_2(GeC), and Ga_2(GeC) nanocages. Improving the thermoelectric efficiency of such materials is achieved by simultaneously increasing the electrical conductance across the highest occupied molecular orbital (HOMO)-lowest unoccupied molecular orbital (LUMO) gap.

Keywords: ion adsorption; B_2(GeC); Al_2(GeC); Ga_2(GeC); DFT.

1. Introduction

Germanium and gallium, which are critical, rare, dispersed metals, have irreplaceable value in various high-tech fields such as fiber-optic communications, infrared optics, semiconductor devices, photovoltaic energy, and biomedical engineering, owing to their unique physical and chemical properties [1].

Boron, aluminum, and gallium are critical supporting elements for global high-tech industries. With increasing resource depletion and stringent environmental requirements, it is imperative to improve resource utilization and achieve clean production globally. The efficient extraction of B, Al, and Ga from solutions is the most important step in industries for these elements. Aqueous solutions containing B, Al, and Ga typically have low concentrations of

these elements and complex chemical compositions, posing challenges for their separation and concentration from the solutions. Therefore, the development of new technologies is of immense significance. Recently, unconventional methods have been performed for the separation of B, Al, and Ga in solutions, including liquid membrane, ionic liquid, ion imprinting, molecular recognition, and functionalized material adsorption technologies [2,3].

It is believed that germanium-based anodes could meet the increasing requirements for batteries with high power and energy densities. The histogram of publications shows increased interest in germanium-based anodes overall over the last decade. Due to its unique Dirac electronic band structure, high room temperature carrier mobility of 230,000 cm2/V s, visible transparency of 97%, exceptional conductivity of 106 S/m, and thermal conductivity of 5000 W/m K, graphene has been used in a variety of industries in areas such as hydrogen storage, electronic devices such as transistors, and field emission displays [4].

With its high specific surface area, graphene has also been used as an electrode material for electrochemical energy devices, including batteries, supercapacitors, fuel cells, and solar cells. The template-assisted in-situ reduction method was used to create the three-dimensional interconnected porous graphene [5–7]. Then, to be employed as anode materials, the Ge nanoparticles were evenly distributed throughout the porous graphene [8,9].

In addition, in medical applications, gallium-based LMs have demonstrated remarkable performance, particularly in antibacterial activity, cancer treatment, and diagnostic imaging, offering unique and more sustainable advantages compared to traditional silver materials [10–12].

As methods effective for constructing carbon-centred chiral spirocycles do not translate to boron and germanium, leaving these chiral centres unexplored, recently, the scientists described a unified strategy for constructing carbon, boron, and germanium-centred chiral spirocyclic skeletons via enantioselective hetero [2+2+2] cycloaddition of a bis-alkyne with a nitrile [13,14].

This investigation aims to delve into the feasibility of B_2(GeC), Al_2(GeC), and Ga_2(GeC) nanoclusters for energy storage. Therefore, the physico-chemical properties of the mentioned heteroclusters of B_2(GeC), Al_2(GeC), and Ga_2(GeC). Following in-depth characterization, samples were measured for their performance correlated with chemical composition variations to assess their potency for B, Al, and Ga in biological cells. What was presented is intended to serve as a basic source of inspiration for addressing the impending scarcity of B, Al, and Ga resources, a challenge that looms on the horizon. This work provides the first DFT-based evaluation of germanium carbide nanocluster for B, Al, Ga coordination and electronic properties. The objectives of this article are to elucidate the intriguing properties associated with the nano-bio-interface of GeC, provide a brief overview of these clusters in advancing nano-biomedicine, and assess their potential as functional components in biomedical applications.

2. Materials and Methods

Figure 1 shows a GeC nanocluster that can adsorb B, Al, or Ga in the biological cells. In this investigation, the computations have been launched by the Coulomb-attenuating method–(Becke, 3-parameter, Lee-Yang-Parr) [CAM–B3LYP–D3] level of theory [15,16].

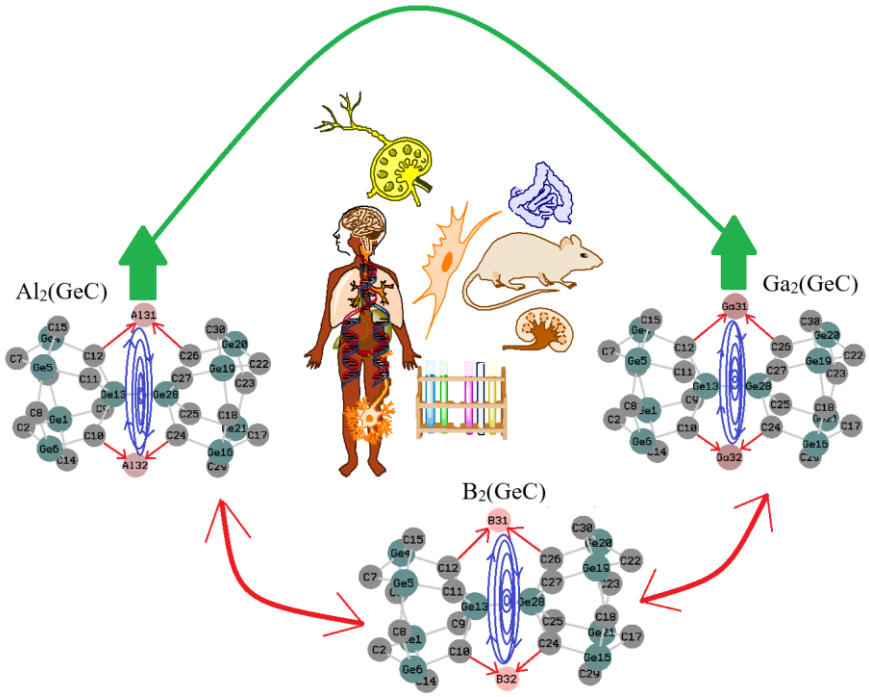

Figure 1. Adding B, Al, Ga to GeC nanocluster and formation of B_2(GeC), Al_2(GeC), and Ga_2(GeC) complexes towards energy storage in novel batteries.

The analysis of Bader charge parameter [17] has been illustrated for hybrid clusters of B_2(GeC), Al_2(GeC), and Ga_2(GeC) (Figure 1) using Gaussian 16 revision C.01 computational software [18] and GaussView 6.1 graphical program [19]. In this research article, the calculations have been done by "CAM–B3LYP–D3" level of theory and basis sets of LANL2DZ for metal atoms and 6–311+G (d,p) for other atoms. Dispersion forces were considered under the "DFT-D3" method of Grimme with Becke–Johnson damping with multiplicity of +1 and convergence on RMS density matrix=1.00D-08 and convergence on MAX density matrix=1.00D-06 [20,21].

One of the most significant advantages of applying GeC nanocluster as the anode in B, Al, or Ga batteries is that they provide several potential B/Al/Ga-ion adsorption sites in a stable GeC anode material, increased electrical conductivity from Ge/C, and surface area from the nanocluster morphology. In this investigation, homogenously distributed germanium or carbon elements can be immobilized in the GeC matrix, which prevents their tendency to form agglomeration under battery cycling. The B /Al/ Ga insertion might also result in the cleavage of some C–B, C–Al, or C–Ga bonds in the GeC anode material and the expansion, providing favorable sites for the subsequent ion insertion in the network (Figure 1a–c). At the same time, the Li, B, Al, or Ga atoms could react rapidly with germanium or carbide of GeC nanocluster to form B_2(GeC), Al_2(GeC), and Ga_2(GeC) heteroclusters. In addition, the implementation and analysis details of computer DFT modeling have explored possible limitations and pitfalls by means of a number of case studies.

3. Results and Discussion

3.1. Charge density differences analysis.

In Figure 2(a–c), charge density differences (CDD) [22] have been shown for B_2(GeC), Al_2(GeC), and Ga_2(GeC) nanoclusters with the vibration in the district about –12 to +9 Bohr through co-interaction between Li31–Li32, and B31– B32, Al31– Al32, Ga31– Ga32.

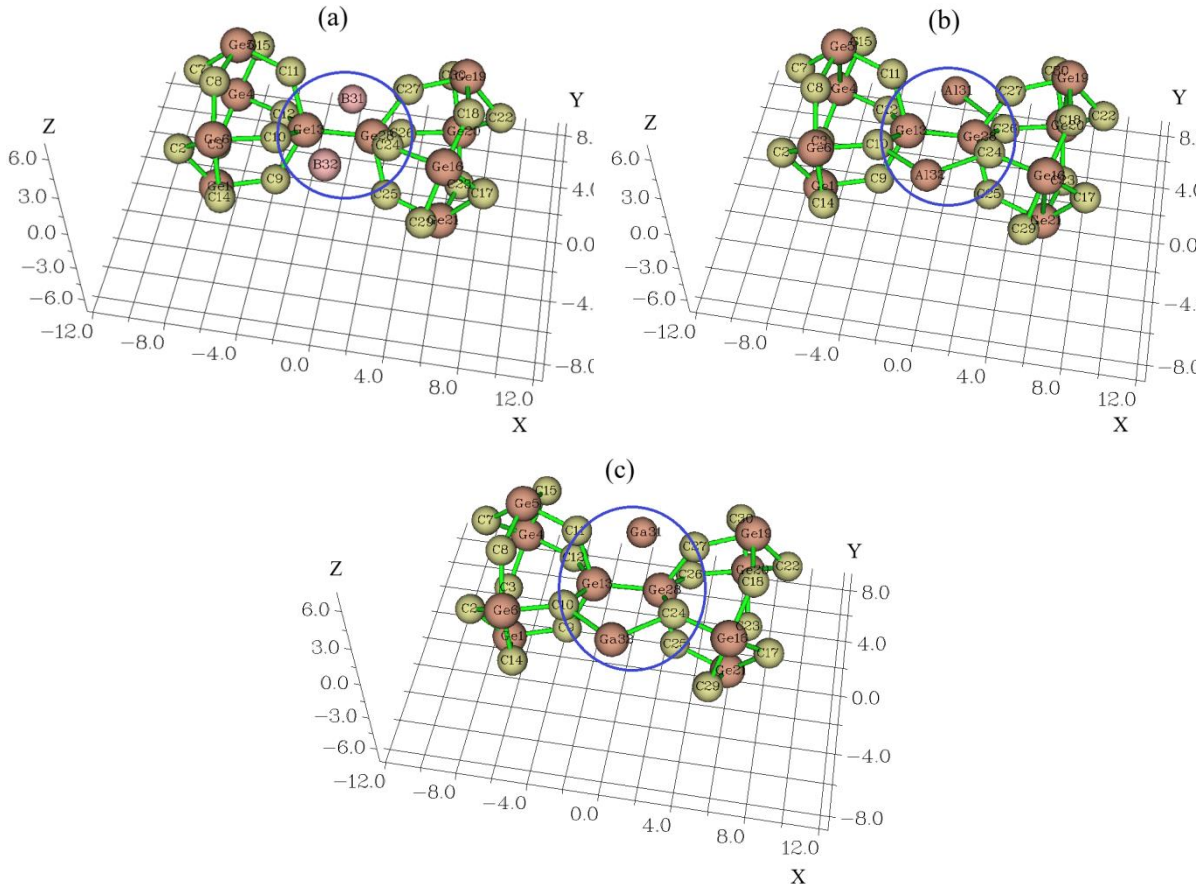

Figure 2. The 3D-CDD graphs for **(a)** B_2(GeC); **(b)** Al_2(GeC); **(c)** Ga_2(GeC) nanoclusters on the X, Y, and Z axes (Bohr).

Moreover, the elements of C2, C3, C7–C12, C14, C15, C17, C18, C22–C27, C29, C30 from B_2(GeC), Al_2(GeC), and Ga_2(GeC) nanoclusters have displayed the vibration about –12 to +9 Bohr (Figure 2a–c).

Electronic metal–carbon interaction plays a fundamental role in tuning the electrocatalytic behavior of the metal active phase. The basis of the metal–nonmetal interaction is the presence of topological and structural defects, as well as the heteroatom functional group silicon, which breaks the perfect symmetry of a graphene layer, providing preferential nucleation and growth sites for metal nanoparticles and a single metal site. As can be seen in Figure 2, the electronic states of carbon sites in GeC near the valence band have an electron acceptor character, while metal ion sites have an electron donor character.

The charge distribution has been illustrated during the atom captured by the GeC nanostructure towards formation of B_2(GeC), Al_2(GeC), and Ga_2(GeC) nanoclusters, respectively (Table 1).

Table 1. The atomic charge (Q/coulomb) for B_2(GeC), Al_2(GeC) and Ga_2(GeC) nanoclusters.

B_2(GeC)		**Al_2(GeC)**		**Ga_2(GeC)**	
Atom	**Q**	**Atom**	**Q**	**Atom**	**Q**
C2	–0.313	C2	–0.310	C2	–0.310
C3	–0.164	C3	–0.160	C3	–0.155
C7	–0.276	C7	–0.279	C7	–0.280
C8	–0.189	C8	–0.172	C8	–0.168
C9	–0.312	C9	–0.277	C9	–0.288
C10	–0.643	C10	–1.084	C10	–1.011
C11	–0.293	C11	–0.259	C11	–0.270
C12	–0.723	C12	–0.970	C12	–0.913
C14	–0.228	C14	–0.230	C14	–0.229
C15	–0.217	C15	–0.227	C15	–0.225

B_2(GeC)		Al_2(GeC)		Ga_2(GeC)	
Atom	**Q**	**Atom**	**Q**	**Atom**	**Q**
C17	–0.322	C17	–0.323	C17	–0.323
C18	–0.175	C18	–0.165	C18	–0.159
C22	–0.272	C22	–0.275	C22	–0.277
C23	–0.172	C23	–0.161	C23	–0.157
C24	–0.671	C24	–1.086	C24	–1.004
C25	–0.274	C25	–0.253	C25	–0.264
C26	–0.642	C26	–0.955	C26	–0.883
C27	–0.416	C27	–0.373	C27	–0.381
C29	–0.206	C29	–0.233	C29	–0.226
C30	–0.228	C30	–0.240	C30	–0.237
B31	0.379	Al31	0.902	Ga31	0.726
B32	0.319	Al32	1.129	Ga32	0.910

Functionalizing of Li, B, Al, Ga atoms can augment the negative atomic charge of C2, C3, C7–C12, C14, C15, C17, C18, C22–C27, C29, C30 as electron acceptors in B_2(GeC), Al_2(GeC), and Ga_2(GeC) nanoclusters (Figure 3a–c).

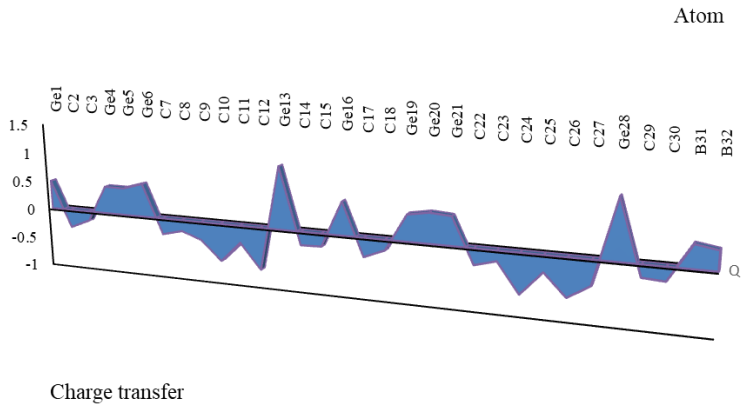

(a)

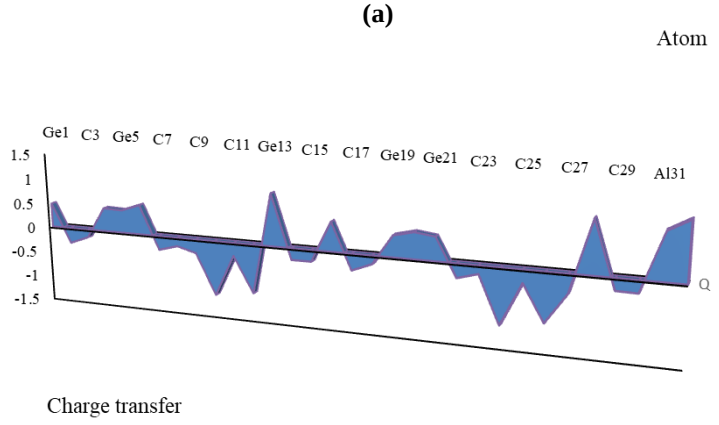

(b)

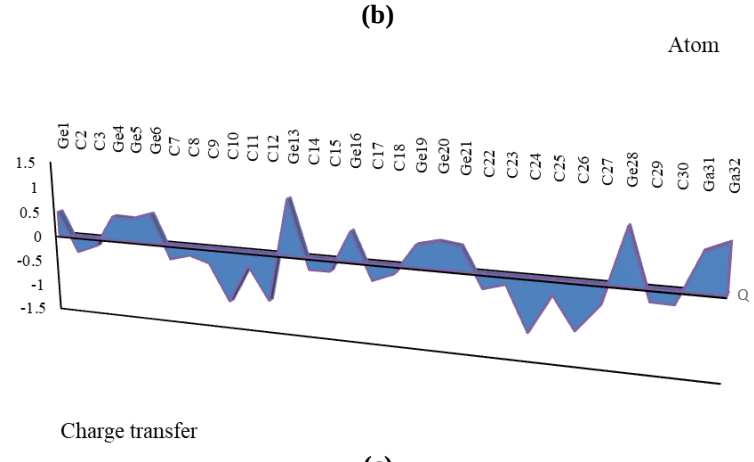

(c)

Figure 3. The changes of charge distribution for **(a)** B_2(GeC); **(b)** Al_2(GeC); **(c)** Ga_2(GeC) nanoclusters.

3.2. Total density of states.

In an isolated system, the energy levels are discrete, and the concept of "density of states (DOS)" is supposed in this situation through the "Multiwfn" program [23,24]. Furthermore, the curve map of "broadened partial DOS (PDOS)" and "overlap DOS (OPDOS)" is valuable for visualizing orbital composition analysis.

Regarding B_2(GeC), Al_2(GeC), and Ga_2(GeC) nanoclusters, TDOS has been evaluated. This factor can demonstrate the existence of important chemical interactions often on the "convex side" (Figure 4a–c).

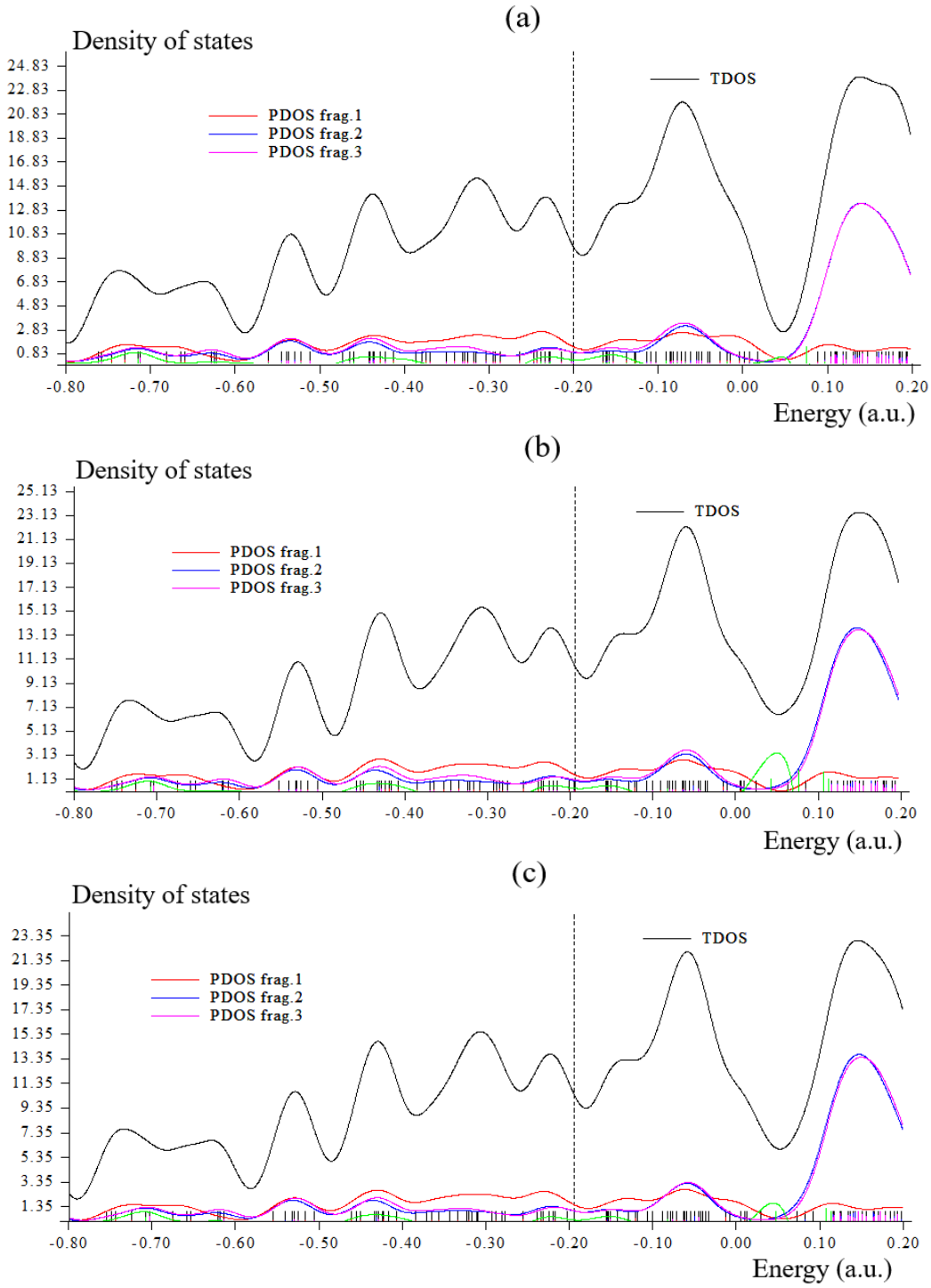

Figure 4. PDOS/TDOS graphs of **(a)** B_2(GeC); **(b)** Al_2(GeC); **(c)** Ga_2(GeC) nanoclusters.

B_2(GeC), Al_2(GeC), Ga_2(GeC) nanoclusters (Figure4a–c) have shown the steepest maximums TDOS surrounding –0.40, –0.50, and –0.60 a.u. owing to the covalent bond

between B, Al, Ga atoms and GeC nanostructure with a maximum density of states of ≈ 12. An analysis of valence bands and Fermi surfaces in both phases indicates that the density of states crucially depends on the parameter in the system's Hamiltonian that controls a topological alternation of the Fermi surface. The signature of that alternation is expected to play an important role in quantities closely related to the density of electronic states, such as charge transport and the optical conductivity of the system.

3.3. Molecular electrostatic potential.

"Molecular electrostatic potential (ESP)" has been commonly used for predicting where nucleophilic and electrophilic reactions might happen for a long time. It is also helpful in understanding hydrogen bonds, halogen bonds, how molecules recognize each other, and how aromatic compounds interact with each other [25]. This function calculates the electrostatic interaction between a single point charge placed at a specific location and the entire system. A positive value means the area is mainly influenced by nuclear charges, while a negative value suggests it's more affected by electronic charges.

Trapping of B, Al, Ga atoms by GeC nanostructure (Figure 5a–c) towards formation of B_2(GeC), Al_2(GeC), and Ga_2(GeC) nanoclusters might be described by ESP graphs using Multiwfn due to achieving their delocalization/localization characterizations of electrons and chemical bonds (Figure 5a–c).

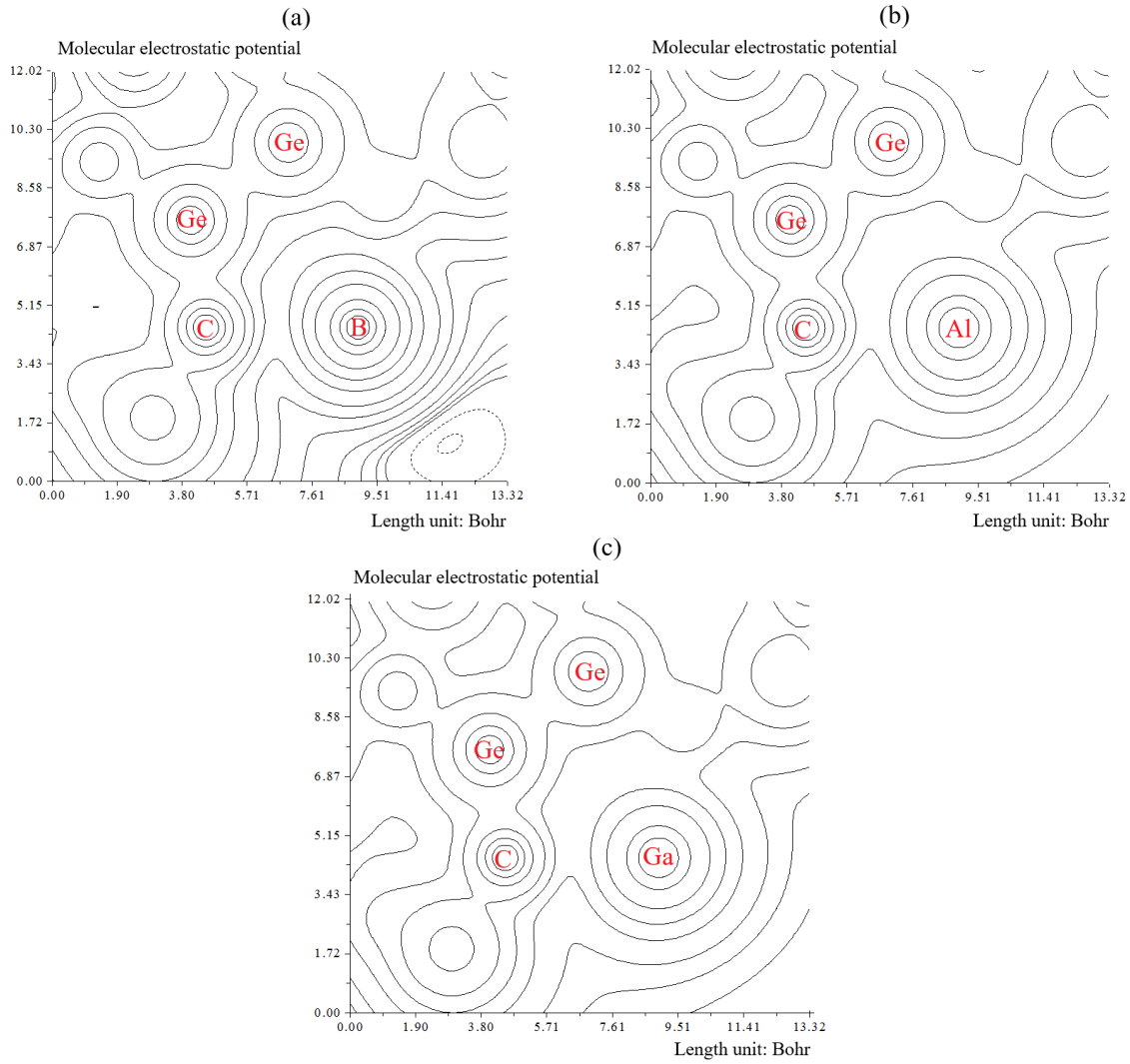

Figure 5. The counter (left side) and shaded (right side) maps of ESP graphs for **(a)** B_2(GeC); **(b)** Al_2(GeC); **(c)** Ga_2(GeC) nanoclusters.

B_2(GeC) (Figure 5a), Al_2(GeC) (Figure 5b), Ga_2(GeC) (Figure 5c) have demonstrated the electron delocalization through an isosurface map with labeling atoms of C10, C12, Si13, C24, C26, Si28, X31/X32 (X= B, Al, Ga). In fact, the counter map of ESP can confirm that B_2(GeC), Al_2(GeC), and Ga_2(GeC) nanoclusters can indicate the ion adsorption in biological cells. (Figure 5a–c). ESP is meaningful in describing features of these potentials and has been utilized to understand the interactive tendencies of molecules in condensed phases. Therefore, it focuses on surface electrostatic potentials and a variety of statistically derived quantities defined in terms of them.

Besides, the intermolecular orbital overlap integral is important in the illustration of intermolecular charge transfer, which can compute HOMO-HOMO and LUMO-LUMO overlap integrals between Li, B, Al, Ga atoms, and GeC nanostructure. The layered germanium carbide doped with boron, aluminum, and gallium has demonstrated structural stability in B-, Al-, and Ga-ion batteries, as indicated by the reported stability energies in Table 2. Improving the thermoelectric efficiency of such materials is achieved by simultaneously increasing the electrical conductance across the highest occupied molecular orbital (HOMO)-lowest unoccupied molecular orbital (LUMO) gap.

Table 2. Stability energy (kcal/mol), dipole moment (debye), LUMO (eV), HOMO(eV), and energy gap (ΔE) (eV) for B_2(GeC), Al_2(GeC), and Ga_2(GeC) nanoclusters.

Heteroclusters	$E_s \times 10^{-3}$ (kcal/mol)	Dipole moment (debye)	E_{HOMO} (eV)	E_{LUMO} (eV)	$\Delta E = E_{LUMO} - E_{HOMO}$ (eV)
B_2(GeC)	-529.5081	0.3377	-5.4430	-4.4901	0.9529
Al_2(GeC)	-500.9893	1.2591	-5.2892	-4.2790	1.0102
Ga_2(GeC)	-501.0702	1.1027	-5.33053	-4.2847	1.0206

Moreover, the intermolecular orbital overlap integral is important in discussions of intermolecular charge transfer, which can calculate HOMO-HOMO and LUMO-LUMO overlap integrals between the metal/metalloids and germanium carbide. The wavefunction level we used was CAM–B3LYP–D3/6–311+G(d,p), which corresponds to HOMO and LUMO, respectively (Table 2). Therefore, E_{LUMO} (a.u.), E_{LUMO} (a.u.), and the local bandgap energies (ΔE/a.u.) and immobile charges induced by polarization discontinuity are simultaneously controlled throughout the structures, and optimized band profiles are eventually achieved for B_2(GeC), Al_2(GeC), and Ga_2(GeC) nanoclusters (Table 2).

The charge surfaces produced at the metal spot, which introduce a dipole in the GeC nanocage, can attach to the surface via ion-quadrupole and ion-induced dipole interactions. The consequences show that the GeC nanocage is appropriate for ion adsorption. These investigations could introduce a perspective on modeling new materials using GeC nanocages for ion separation.

4. Conclusions

Metal/metalloid atom capture by germanium carbide towards the formation of B_2(GeC), Al_2(GeC), and Ga_2(GeC) nanoclusters was studied by computational methods. The changes of charge density are defined as a notable charge transfer in B_2(GeC), Al_2(GeC), and Ga_2(GeC). Due to the semiconducting nature of GeC, it is usually composited with C for better ionic and electronic conductivities. This research article demonstrates the use of high-power-density/energy-density materials to separate B, Al, or Ga in biological cells, with excellent cycle stability. The treatment of methods increases in complexity and experimental challenges: from lysates and fluids to cells and tissues, to living cells and animals, and finally to the

prospects of applying extant technology to investigations in body cells. Computational design can be used to establish a surface-state model of the interaction between the GeC nanocage and ion separation in the body, ensuring safety and effectiveness. Therefore, future research should pay more attention to theoretical simulations to accurately and in-depth study nano-bio-interactions, paving the way for safe and effective biomedical applications of GeC nanocage bio-interface.

Author Contributions

Conceptualization, F.M.; methodology, F.M.; software, F.M.; validation, F.M. and M.M.; formal analysis, F.M. and M.M.; investigation, F.M. and M.M.; resources, F.M. and M.M.; data curation, F.M.; writing—original draft preparation, F.M.; writing—review and editing, M.M.; visualization, F.M. and M.M.; supervision, F.M.; project administration. The authors have read and agreed to the published version of the manuscript.

Institutional Review Board Statement

Not applicable.

Informed Consent Statement

Not applicable.

Data Availability Statement

Not applicable.

Funding

This research received no funding.

Acknowledgments

In successfully completing this paper and its research, the authors are grateful to Kastamonu University.

Conflict of Interest

The authors declare no conflict of interest.

Reference

1. Guan, T.; Guo, M.; Wang, L.; Liu, J. Production and recycling of the cutting edge material of gallium: A review. *Sci. Total Environ.* **2025**, *971*, 179046, https://doi.org/10.1016/j.scitotenv.2025.179046.
2. Teng, D.; Wu, J.; Ma, Q.; Wang, W.; Zhou, G.; Fan, G.; Cao, Y.; Li, P. Advances in the Recovery of Critical Rare Dispersed Metals (Gallium, Germanium, Indium) from Urban Mineral Resources. *ACS Omega* **2025**, *10*, 76-92, https://doi.org/10.1021/acsomega.4c08689.
3. Liang, Y.; Luo, B.; Zhao, L.; Chen, L.; Ding, B.; Shen, Z.; Zheng, T.; Guo, Y.; Li, Q.; Zhou, B.; Liu, C.; Brnic, J.; Ren, W.; Zhong, Y. Strong magnetic and ultrasonic fields enhanced the leaching of Ga and Ge from zinc powder replacement residue. *Sep. Purif. Technol.* **2024**, *330*, 125572, https://doi.org/10.1016/j.seppur.2023.125572.
4. Mollaamin, F. Anchoring of 2D layered materials of $Ge_5Si_5O_{20}$ for (Li/Na/K)-(Rb/Cs) batteries towards Eco-friendly energy storage. *BMC Chem.* **2025**, *19*, 233, https://doi.org/10.1186/s13065-025-01593-0.

5. Mollaamin, F. Competitive Intracellular Hydrogen-Nanocarrier Among Aluminum, Carbon, or Silicon Implantation: a Novel Technology of Eco-Friendly Energy Storage using Research Density Functional Theory. *Russ. J. Phys. Chem. B.* **2024**, *18*, 805–820, https://doi.org/10.1134/S1990793124700131.
6. AlJaber, G.; AlShammari, B.; AlOtaibi, B. From Theory to Experiment: Reviewing the Role of Graphene in Li-Ion Batteries Through Density Functional Theory. *Nanomaterials* **2025**, *15*, 992, https://doi.org/10.3390/nano15130992.
7. Yin, S.; Zhang, X.; Huang, X.; Zhou, F.; Wang, Y.; Wen, G. SnO/SnO_2 Heterojunction Nanoparticles Anchored on Graphene Nanosheets for Lithium Storage. *ACS Appl. Nano Mater.***2024**, *7*, 14419-14430, https://doi.org/10.1021/acsanm.4c01720.
8. Politano, G.G. Optical Properties of Graphene Nanoplatelets on Amorphous Germanium Substrates. *Molecules* **2024**, *29*, 4089, https://doi.org/10.3390/molecules29174089.
9. Zhao, M.; Xue, Z.; Zhu, W.; Wang, G.; Tang, S.; Liu, Z.; Guo, Q.; Chen, D.; Chu, P.K.; Ding, G.; Di, Z. Interface Engineering-Assisted 3D-Graphene/Germanium Heterojunction for High-Performance Photodetectors. *ACS Appl. Mater. Interfaces* **2020**, *12*, 15606-15614, https://doi.org/10.1021/acsami.0c02485.
10. Chai, J.; Mao, Z.; Wang, R. Functional additives for $AlCl_3$/EMIC ionic liquid electrolyte of rechargeable aluminum batteries: advancements and challenges. *Energy Storage Mater.* **2025**, *81*, 104475, https://doi.org/10.1016/j.ensm.2025.104475.
11. Mollaamin, F.; Monajjemi, M. Electric and Magnetic Evaluation of Aluminum–Magnesium Nanoalloy Decorated with Germanium Through Heterocyclic Carbenes Adsorption: A Density Functional Theory Study. *Russ. J. Phys. Chem. B* **2023**, *17*, 658–672, https://doi.org/10.1134/S1990793123030223.
12. Fu, M.; Shen, Y.; Zhou, H.; Liu, X.; Chen, W.; Ma, X. Gallium-based liquid metal micro/nanoparticles for photothermal cancer therapy. *J. Mater. Sci. Technol.* **2023**, *142*, 22-33, https://doi.org/10.1016/j.jmst.2022.08.049.
13. Cao, Y.-X.; Chauvin, A.-S.; Tong, S.; Alama, L.; Cramer, N. Accessing carbon, boron and germanium spiro stereocentres in a unified catalytic enantioselective approach. *Nat. Catal.* **2025**, *8*, 569-578, https://doi.org/10.1038/s41929-025-01352-3.
14. Zhang, L.; Cui, Z. Theoretical Study on Electronic, Magnetic and Optical Properties of Non-Metal Atoms Adsorbed onto Germanium Carbide. *Nanomaterials* **2022**, *12*, 1712, https://doi.org/10.3390/nano12101712.
15. Becke, A.D. Density-functional thermochemistry. III. The role of exact exchange. *J. Chem. Phys*. **1993**, *98*, 5648–5652, https://doi.org/10.1063/1.464913.
16. Lee, C.; Yang, W.; Parr, R.G. Development of the Colle-Salvetti correlation-energy formula into a functional of the electron density. *Phys. Rev. B* **1988**, *37*, 785, https://doi.org/10.1103/PhysRevB.37.785.
17. Xie, L.; Wang, J.; Wang, K.; He, Z.; Liang, J.; Lin, Z.; Wang, T.; Cao, R.; Yang, F.; Cai, Z. Modulating the Bader Charge Transfer in Single *p*-Block Atoms Doped Pd Metallene for Enhanced Oxygen Reduction Electrocatalysis. *Angew. Chem., Int. Ed.* **2024**, *63*, e202407658, https://doi.org/10.1002/ange.202407658.
18. Frisch, M.J.; Trucks, G.W.; Schlegel, H.B.; Scuseria, G.E.; Robb, M.A.; Cheeseman, J.R.; Scalmani, G.; Barone, V.; Petersson, G.A.; Nakatsuji, H.; Li, X.; Caricato, M.; Marenich, A.V.; Bloino, J.; Janesko, B.G.; Gomperts, R.; Mennucci, B.; Hratchian, H.P.; Ortiz, J. V.; Izmaylov, A. F.; Sonnenberg, J.L.; Williams-Young, D.; Ding, F.; Lipparini, F.; Egidi, F.; Goings, J.; Peng, B.; Petrone, A.; Henderson, T.; Ranasinghe, D.; Zakrzewski, V.G.; Gao, J.; Rega, N.; Zheng, G.; Liang, W.; Hada, M.; Ehara, M.; Toyota, K.; Fukuda, R.; Hasegawa, J.; Ishida, M.; Nakajima, T.; Honda, Y.; Kitao, O.; Nakai, H.; Vreven, T.; Throssell, K.; Montgomery, J.A., Jr.; Peralta, J.E.; Ogliaro, F.; Bearpark, M.J.; Heyd, J.J.; Brothers, E.N.; Kudin, K.N.; Staroverov, V.N.; Keith, T.A.; Kobayashi, R.; Normand, J.; Raghavachari, K.; Rendell, A.P.; Burant, J.C.; Iyengar, S.S.; Tomasi, J.; Cossi, M.; Millam, J.M.; Klene, M.; Adamo, C.; Cammi, R.; Ochterski, J.W.; Martin, R.L.; Morokuma, K.; Farkas, O.; Foresman, J.B.; Fox, D.J. Gaussian 16, Revision C.01, Gaussian, Inc., Wallingford CT, **2016**.
19. Dennington, R.; Keith Todd, A.; Millam John, M. GaussView, Version 6.06.16. Semichem Inc., Shawnee Mission, KS, USA, **2016**.
20. Mollaamin, F.; Monajjemi, M. Adsorption ability of Ga_5N_{10} nanomaterial for removing metal ions contamination from drinking water by DFT. *Int. J. Quantum Chem.* **2024**, *124*, e27348, https://doi.org/10.1002/qua.27348.
21. Kohn, W.; Sham, L.J. Self-Consistent Equations Including Exchange and Correlation Effects. *Phys. Rev.* **1965**, *140*, A1133, https://doi.org/10.1103/PhysRev.140.A1133.

22. Xu, Z.; Qin, C.; Yu, Y.; Jiang, G.; Zhao, L. First-principles study of adsorption, dissociation, and diffusion of hydrogen on α-U (110) surface. *AIP Adv.* **2024**, *14*, 055114, https://doi.org/10.1063/5.0208082.
23. Lu, T.; Chen, F. Multiwfn: A multifunctional wavefunction analyzer. *J. Comput. Chem.* **2012**, *33*, 580-592, https://doi.org/10.1002/jcc.22885.
24. Lu, T. A comprehensive electron wavefunction analysis toolbox for chemists, Multiwfn. *J. Chem. Phys.* **2024**, *161*, 082503, https://doi.org/10.1063/5.0216272.
25. Murray, J.S.; Riley, K.E.; Brinck, T. A Revival of Molecular Surface Electrostatic Potential Statistical Quantities: Ionic Solids and Liquids. *Crystals* **2024**, *14*, 995, https://doi.org/10.3390/cryst14110995.

Publisher's Note & Disclaimer